

Answer Questions with Right Image Regions: A Visual Attention Regularization Approach

YIBING LIU, YANGYANG GUO, JIANHUA YIN, and XUEMENG SONG, Shandong University, China
 WEIFENG LIU, China University of Petroleum (East China), China
 LIQIANG NIE, Shandong University, China

Visual attention in Visual Question Answering (VQA) targets at locating the right image regions regarding the answer prediction. However, recent studies have pointed out that the highlighted image regions from the visual attention are often irrelevant to the given question and answer, leading to model confusion for correct visual reasoning. To tackle this problem, existing methods mostly resort to aligning the visual attention weights with human attentions. Nevertheless, gathering such human data is laborious and expensive, making it burdensome to adapt well-developed models across datasets. To address this issue, in this paper, we devise a novel visual attention regularization approach, namely AttReg, for better visual grounding in VQA. Specifically, AttReg firstly identifies the image regions which are essential for question answering yet unexpectedly ignored (*i.e.*, assigned with low attention weights) by the backbone model. And then a mask-guided learning scheme is leveraged to regularize the visual attention to focus more on these ignored key regions. The proposed method is very flexible and model-agnostic, which can be integrated into most visual attention-based VQA models and require no human attention supervision. Extensive experiments over three benchmark datasets, *i.e.*, VQA-CP v2, VQA-CP v1, and VQA v2, have been conducted to evaluate the effectiveness of AttReg. As a by-product, when incorporating AttReg into the strong baseline LMH, our approach can achieve a new state-of-the-art accuracy of 59.92% with an absolute performance gain of 6.93% on the VQA-CP v2 benchmark dataset. In addition to the effectiveness validation, we recognize that the faithfulness of the visual attention in VQA has not been well explored in literature. In the light of this, we propose to empirically validate such property of visual attention and compare it with the prevalent gradient-based approaches.

CCS Concepts: • **Computing methodologies** → **Computer vision tasks**; *Computer vision representations*; • **Information systems** → *Question answering*.

Additional Key Words and Phrases: Visual question answering, mask-guided learning, visual attention regularization.

ACM Reference Format:

Yibing Liu, Yangyang Guo, Jianhua Yin, Xuemeng Song, Weifeng Liu, and Liqiang Nie. 2021. Answer Questions with Right Image Regions: A Visual Attention Regularization Approach. *ACM Trans. Multimedia Comput. Commun. Appl.* 0, 0, Article 0 (2021), 16 pages. <https://doi.org/00.0000/0000000.0000000>

Y. Liu, Y. Guo, J. Yin, X. Song, and L. Nie are with the School of Computer Science and Technology, Shandong University, 72 Binhai Road, Jimo, Qingdao, Shandong Province, China (266237); emails: lyibing112@gmail.com, guoyang.eric@gmail.com, jhyin@sdu.edu.cn, sxmusc@gmail.com, nieliqiang@gmail.com; J. Yin and L. Nie are the corresponding authors (emails: jhyin@sdu.edu.cn, nieliqiang@gmail.com); W. Liu is with the College of Control Science and Engineering, China University of Petroleum (East China), 66 West Changjiang Road, Huangdao District, Qingdao, Shandong Province, China (266580); email: liuwf@upc.edu.cn.

Permission to make digital or hard copies of all or part of this work for personal or classroom use is granted without fee provided that copies are not made or distributed for profit or commercial advantage and that copies bear this notice and the full citation on the first page. Copyrights for components of this work owned by others than ACM must be honored. Abstracting with credit is permitted. To copy otherwise, to republish, to post on servers or to redistribute to lists, requires prior specific permission and/or a fee. Request permissions from permissions@acm.org.

© 2021 Association for Computing Machinery.

1551-6857/2021/0-ART0 \$15.00

<https://doi.org/00.0000/0000000.0000000>

1 INTRODUCTION

Visual Question Answering (VQA) aims to correctly answer natural language questions about an image. As an “AI-complete” problem, VQA encounters a variety of research challenges such as recognition, counting, and multi-step reasoning, to name a few. Canonical methods often cast VQA as a classification task [2, 3, 5, 11, 12, 16–18, 30–32], where the image and question are processed via Convolutional Neural Networks (CNNs) and Recurrent Neural Networks (RNNs), respectively. Among the existing methods, an intriguing design is to apply the visual attention mechanism to image regions based on the given question, equipping VQA models with the capability of visual grounding and explanation.

Generally speaking, the visual attention in VQA executes an explicit step of identifying “where to look” [27, 29]. To be more specific, it allows the model to assign distinctive weights to different image regions, which are computed via the semantic similarity between the given question and image features, as illustrated in Figure 1. Similar to human vision systems, the image regions with high attention weights are commonly deemed as where the model looks at when making decisions. Accordingly, by spotting such relevant image regions, the visual attention is able to not only reduce noisy features but also construct more refined visual representations.

Despite of the fact that existing VQA models have benefited a lot from the visual attention, one imperative issue lies in the lack of guidance for visual grounding. This often leads visual attention mechanisms to focus on image regions which are less relevant to the correct answer [10, 26]. As shown in Figure 1, the visual attention in the backbone model focuses on the much less important region *dog* while ignores the most relevant one *frisbee*, misleading the model to predict the incorrect answer *brown*. To deal with this issue, a seemingly straightforward solution is to align visual attention weights with explicit human attentions [21, 34]. Collecting such data is, however, expensive and difficult [10], thereby limiting the practicality of this kind of approach.

Orthogonal to the visual attention, Gradient-weighted Class Activation Mapping (Grad-CAM [25]) methods leverage the gradient value of each image region according to the model prediction results to accomplish the task of visual grounding. For instance, the method in [26] calculates the gradient of each image region according to the ground-truth answers, and encourages the rank consistency between the gradients and human attentions for better visual grounding. More recently, Wu and Mooney [28] utilized the textual annotations (e.g., QA pairs) as auxiliary information and regularize visual grounding by penalizing the gradients of important regions to wrong answers. However, our experiments reveal that such gradient-based methods are not trustworthy for visual grounding compared with that of visual attention. One notable problem is that the image regions with large gradient-based weights are not closely relevant to the answer prediction, which violates the intuition that Grad-CAM is specially designed for better visual grounding in VQA [26].

To overcome the limitations of previous approaches, in this paper, we present a novel visual attention regularization method, dubbed as AttReg, to guide the learning of visual attention in VQA. As illustrated in Figure 1, AttReg aims to achieve better accuracy via attention weights regularization. Specifically, for each training sample, AttReg firstly identifies the ignored key regions, i.e., the image regions pivotal to the question answering but assigned with low attention weights. Thereafter, AttReg builds another sample composed of the same question and a new curated image with these ignored key regions being masked. Crucially, the model is trained to answer *None* when given the curated sample since the relevant image regions are masked and invisible under this situation. By refraining the curated samples from being correctly answered, these ignored key regions are guided to yield stronger influence towards model predictions, thereby the model is regularized to attach higher attention weights to them and boosting the answer prediction accuracy. In a nutshell, our end-to-end approach is simple to implement, which requires

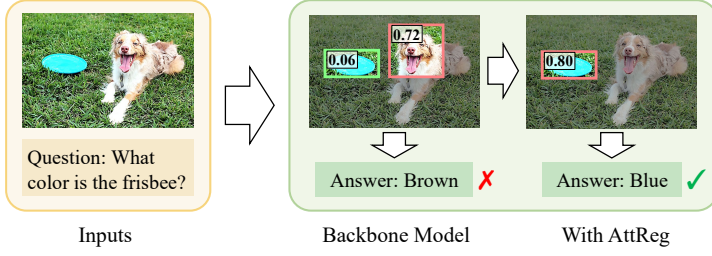


Fig. 1. Demonstration of the visual attention in VQA and our regularization method. The green box (*i.e.*, *frisbee*) in the middle image denotes the key region ignored by the backbone visual attention mechanism, wherein lower attention weight is assigned compared to the pink box (*i.e.*, *dog*). In the rightmost image, our AttReg regularizes the attention map to focus more on the most relevant *frisbee* region.

no human supervision and can be applied to most of the existing visual attention-based VQA models. We conduct extensive experiments on three VQA datasets, *i.e.*, VQA-CP v1 [1], VQA-CP v2 [1], and VQA v2 [13], to verify the effectiveness of the proposed method. Experimental results have shown that our proposed method is capable of guiding the visual attention learning, and enhancing the performance of many visual attention-based VQA models.

In addition to the effectiveness validation, the faithfulness of the visual attention in VQA has not been well explored so far. The faithfulness here refers to the consistency between the attention weight and the contribution of its corresponding image region to model decisions. In particular, weak faithfulness can be obtained if the regions with high attention weights often have little influence on model predictions. To justify such a property, we empirically conduct occlusion studies [25] on a well-devised visual attention model – UpDn [2]. we notice that the auto-learned attention weight is highly correlated with the influence of image regions towards model decisions, which demonstrates the favorable faithfulness of visual attention.

In summary, the contributions of this work are three-fold:

- We present a novel visual attention regularization method in VQA, which is able to guide the model towards correctly answering questions based on right image regions. The proposed regularization approach is model-agnostic, requiring no human attention supervision, and can be incorporated into most visual attention-based VQA models, such as UpDn and LMH [9].
- We empirically study the faithfulness of prevalent visual attention in VQA. The results exhibit that the visual attention is more faithful to model decisions in comparison with the Grad-CAM methods.
- Extensive experiments demonstrate that the proposed method can simultaneously improve the visual grounding accuracy and the backbone model performance. As a side product, by introducing our regularization method to a strong model LMH, we can achieve a new state-of-the-art performance over the VQA-CP v2 dataset. We have released the involved data, codes, and parameter settings to facilitate other researchers in this community¹.

The remainder of this paper is organized as follows. In Section 2, we study the faithfulness of the visual attention mechanism and compare it with the Grad-CAM methods. Section 3 details the visual attention in VQA and our proposed method. Experimental settings and results are illustrated

¹<https://github.com/BierOne/VQA-AttReg>.

Table 1. Accuracy of UpDn on two datasets, VQA v2 and VQA-CP v2. Gap Δ denotes the performance variation in comparison with the baseline.

Method	VQA v2		VQA-CP v2	
	Overall	Gap Δ	Overall	Gap Δ
<i>Baseline using full image features</i>				
UpDn	63.97	-	40.33	-
<i>Visual attention</i>				
Maintain highest _{10%}	62.89	-1.08	40.40	+0.07
Maintain highest _{20%}	63.42	-0.55	40.47	+0.14
Maintain lowest _{10%}	38.92	-25.05	22.07	-18.26
Maintain lowest _{20%}	40.38	-23.59	22.03	-17.30
<i>Grad-CAM</i>				
Maintain highest _{10%}	52.03	-11.94	35.33	-5.00
Maintain highest _{20%}	52.96	-11.01	35.66	-4.67
Maintain lowest _{10%}	56.98	-6.99	33.99	-6.34
Maintain lowest _{20%}	57.88	-6.09	34.35	-5.98

in Section 4, followed by the related work in Section 5. The conclusion and future works are presented in Section 6.

2 VISUAL ATTENTION FAITHFULNESS EXPLORATION

One intuitive property in visual attention is that the image regions with larger attention weights should contribute more to model decisions, since these regions represent where the model focuses on when making decisions. For clarity, here we define this property as the faithfulness of visual attention. To justify it, we conduct occlusion studies and quantify the contribution of each image region via two measurement: performance change and prediction variation.

2.1 Contribution to model performance

We empirically characterize visual attention weights as the contribution of image regions towards model performance, and measure the performance change when using different portions of image features². As shown in Table 1, when images merely maintain the 20% highest attention weights of regions, the model can obtain very comparative results with the baseline using full image features, e.g., the performance only drops 0.55% on VQA v2. Moreover, we further examine the model performance when only maintaining the 10% or 20% lowest attention weights of image regions. As can be expected, the performance of the model largely drops compared with the baseline.

In addition, we leverage the same setting to testify the faithfulness of the Grad-CAM method. Table 1 demonstrates that the model performance of maintaining the relatively lowest gradient weights of image regions is very close to and even superior to the one with the relatively highest gradient weights, which is confusing since regions with larger gradients in Grad-CAM should contribute more to the model performance. In contrast, the visual attention weight shows a more acceptable consistency in model performance change.

Finally, we report the model performance when maintaining image features of each attention (or gradient) weight interval, e.g., 10%-20% highest ones. As can be seen in Figure 2 (a), the model

²Note that the image features we used are composed of 36 object proposal features extracted by Faster R-CNN.

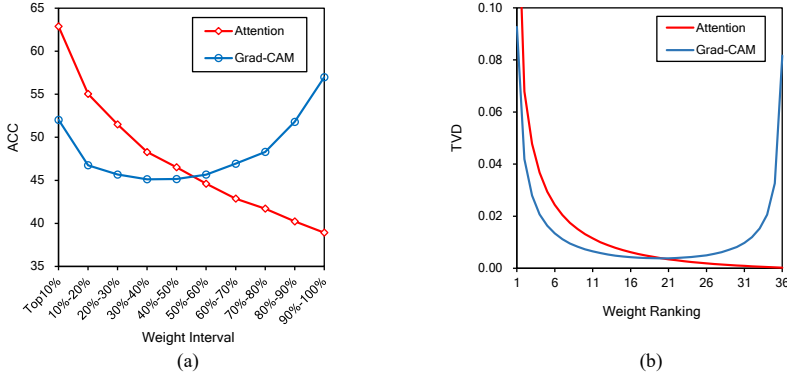


Fig. 2. Faithfulness evaluation. (a) Performance curve regarding the weight intervals. (b) The TVD value with respect to weight ranking.

performance continuously declines as the attention weights of the maintained regions decrease. In contrast, by employing Grad-CAM as the visual grounding, the model performance drops first and then improves with the descending of the maintained weights. This finding further verifies our previous observation in Table 1 that the visual attention is more faithful than Grad-CAM pertaining to visual grounding.

2.2 Contribution to model prediction

To study the relationship between the attention weight and the contribution of the image region to model prediction, we further remove each region sequentially according to its assigned weight value and observe the prediction variation. Specifically, the region contribution is quantified through the prediction variation with and without the current image region, which is expressed by the Total Variation Distance (TVD) [15],

$$\text{TVD}(p_1, p_2) = \frac{1}{2} \sum_i |p_{1i} - p_{2i}|, \quad (1)$$

where p_1 and p_2 represent two different sets of predicted scores for each answer, respectively. A higher TVD denotes that the tested region is more influential for answer prediction.

We have computed the TVD for each image region with respect to its ranked weight and plotted the results in Figure 2 (b). It can be found that the TVD is monotonously decreasing along the descending of the ranked attention weight, which demonstrates the tight correlation between the attention weight and region contribution towards answer prediction. In contrast, many regions with a very low ranking of Grad-CAM weights (*i.e.*, ranking 26 to 36) yield a strong influence for answer prediction, which is confusing and violates the visual-grounding ability of Grad-CAM to some extent.

Based on the above experiments, we can conclude that the visual attention provides a more satisfactory testbed for visual grounding than Grad-CAM in VQA. Nevertheless, some key objects are still ignored by the visual attention as observed in our experiment, as shown in Figure 4 (b). Inspired by this, we intend to develop a more advanced and pluggable approach to regularizing the visual attention, which can effectively promote the backbone model performance.

3 APPROACH

Our approach aims at regularizing VQA models to predict the right answers based on the right image regions. In the following, we first state the basic knowledge of VQA and its visual attention variant in Sec. 3.1. The details of the proposed method are then elaborated in Sec. 3.2.

3.1 Preliminaries

3.1.1 Problem Formulation. The goal of VQA is to provide a correct answer \hat{A} to a given textual question Q upon an image I . And the common function of VQA is formulated as a classification problem:

$$\hat{A} = \arg \max_{A_j \in \mathcal{A}} P(A_j | Q, I; \Theta), \quad (2)$$

where \mathcal{A} denotes the candidate answer set and Θ denotes all the model parameters.

3.1.2 Visual Attention in VQA (VAtt). Traditional visual attention mechanisms used in VQA models are of the top-down fashion, which directly recognize relevant image regions over the convolutional features. The complementary bottom-up attention mechanism is therefore proposed to detect objects and attributes in images for identifying high-level concepts [2]. In this subsection, we mainly recap the bottom-up and top-down (UpDn) attention model.

As illustrated in Algorithm 1, for each image I , the UpDn model utilizes the object detection techniques (e.g., Faster R-CNN [23]) to extract a object feature set $\mathcal{V} = \{v_k\}_{k=1}^K$. And for each question Q , a RNN (e.g., GRU [8]) is used to capture the sequential features represented by q , i.e. $q = \text{RNN}(Q)$. The visual attention mechanism is then utilized to refine visual representations by employing the question feature to attend on each object in the image,

$$\begin{cases} s_i = w_a^T f_a([v_i, q]), \\ \alpha = \text{softmax}(s), \end{cases} \quad (3a)$$

$$\quad (3b)$$

$$\begin{cases} \hat{v} = \sum_{i=1}^K \alpha_i v_i, \end{cases} \quad (3c)$$

where α and s respectively denote the attention weights and the computed scores for image objects, w_a is a trainable parameter vector, $f_a(\cdot)$ denotes the fusion function, and \hat{v} is the final visual representation. The weighted visual feature \hat{v} and the question feature q are then fed into the answer prediction module f_p to predict the confidence for all candidate answers,

$$p = f_p(\hat{v}, q). \quad (4)$$

In fact, each question may have several correct answers due to the differentiation in human annotators. Hence, the model prediction is supervised by a set of soft values $y \in [0, 1]^{|A|}$, where y_j denotes the occurrence probability of the candidate answer A_j based on the human labeled answers. Specifically, UpDn adopts the binary-cross-entropy loss to optimize the model parameters,

$$\mathcal{L} = \sum_i \sum_j y_{ij} \log(p_{ij}) - (1 - y_{ij}) \log(1 - p_{ij}), \quad (5)$$

where the indices i and j refer to the training questions and candidate answers, respectively.

3.2 Visual Attention Regularization (AttReg)

Existing VQA models often make mistakes due to the inappropriate visual grounding. To tackle this issue, in this work, we regularize the visual attention for better model performance. As shown in Figure 3, given a training sample $\langle Q, I, \hat{A} \rangle$, we first identify the ignored key objects and construct

Algorithm 1 Typical Visual Attention-based Model (UpDn)

```

1: function UpDn( $I, Q, \hat{A}$ )
2:    $\mathcal{V} \leftarrow \text{RCNN}(I), \quad q \leftarrow \text{RNN}(Q)$  ▷ image features and question features
3:    $\alpha \leftarrow \text{VAtt}(\mathcal{V}, q)$  ▷ visual attention weights
4:    $\hat{v} \leftarrow \sum_{i=1}^K \alpha_i v_i$  ▷ final visual representation
5:    $p \leftarrow f_p(\hat{v}, q)$  ▷ predicted probabilities for all candidate answers
6:   Compute soft values  $y$  for ground-truth answers  $\hat{A}$ 
7:   Compute loss  $\mathcal{L}$  according to Eqn. (5)
8:   return  $\alpha, \mathcal{L}$ 
9: end function

```

Algorithm 2 Visual Attention Regularization (AttReg)

```

1: function AttReg( $I, Q, \hat{A}$ )
2:    $V^* \leftarrow$  key objects identification
3:    $\alpha, \mathcal{L}_{vqa} \leftarrow \text{UpDn}(I, Q, \hat{A})$  ▷ original training sample
4:    $V^o \leftarrow$  ignored objects localization
5:    $I^m \leftarrow$  masking ignored key objects ( $V^* \cap V^o$ ) in  $I$ 
6:    $\hat{A}^m := \emptyset$ 
7:    $\neg, \mathcal{L}_{reg} \leftarrow \text{UpDn}(I^m, Q, \hat{A}^m)$  ▷ curated training sample
8:    $\mathcal{L}_{all} \leftarrow \mathcal{L}_{vqa} + \lambda \mathcal{L}_{reg}$  ▷ parameter update
9: end function

```

a new curated image I^m with these objects being masked. Then we append a complementary sample $\langle Q, I^m, \hat{A}^m \rangle$ to regularize the model for better attention learning. The following will sequentially introduce these two procedures of AttReg.

3.2.1 Curated-Image Construction. The module of curated-image construction consists of three main steps: (i) identifying key objects related to the QA pair, represented as V^* ; (ii) locating ignored objects through visual attention, represented as V^o ; (iii) masking the ignored key objects (*i.e.*, $V^* \cap V^o$) and constructing a new curated image I^m .

Particularly, we firstly take the QA pair as the auxiliary information to determine the importance of each object in the image. Following [28], we assign POS tags to each word in the QA using the spaCy POS tagger [14] and extract nouns in the QA. Thereafter, we calculate the cosine similarity between the GloVe [20] embedding of object categories and the extracted nouns. The top- M objects with the highest similarity scores are selected as key objects V^* . We consider these objects as essential since they are highly related to the QA. Note that directly leveraging these extracted key objects as the supervision is sub-optimal as studied in prior work [26]. The dominant reason is that the presence of superficial linguistic correlations (*i.e.*, language biases [13, 33]) can easily mislead the model to ignore visual content even under a strong supervision [26]. In the light of this, we instead apply these key objects to compose a new training sample, which can help the model build correlation between the right visual information and the ground-truth answer. The superficial bias can also be alleviated to some extent.

Secondly, we take the visual attention weights α as the evaluation standard for examining the influence of each object towards model decisions. As mentioned in Table 1, remaining merely $N\%$ (*e.g.*, 20%) image objects with the highest attention weights can achieve very competitive performance (63.42% vs. 63.97%), which implies that most image objects out of top- $N\%$ hardly

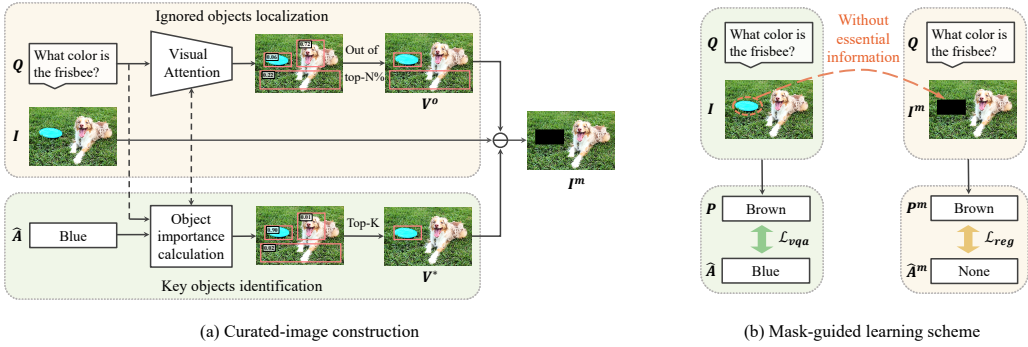


Fig. 3. Illustration of the proposed AttReg for regularizing the visual attention. (a) Given a training sample, a curated-image is firstly constructed by masking the identified ignored key objects. (b) The AttReg then composes a new training sample to regularize the visual attention to focus more on the ignored key objects.

impose an effect on the model predictions. Consequently, to avoid trivial procedures, we directly select image objects that are out of top- $N\%$ attention weight rank as the ignored objects V^o .

Lastly, we use the intersection of V^* and V^o as the ignored key objects and mask them in the original image I to construct a new curated image I^m .

3.2.2 Mask-guided Learning Scheme. Based on the curated image I^m , we then design a mask-guided learning scheme to regularize the model, which emphasizes more on the ignored key objects towards question answering. We argue that a VQA model cannot correctly answer the question if it is blind to the key objects from the given image. In a sense, the curated image I^m lacks essential visual information in correctly answering the question Q because the key objects are masked. We hence simply zero-out all ground-truth answers in \hat{A} for $\langle Q, I^m \rangle$ and compose a new training sample $\langle Q, I^m, \hat{A}^m \rangle$, i.e., \hat{A}^m is \emptyset . In this way, the devised mask-guided learning scheme enforces the variation in the target answer distribution when the training image loses the ignored key objects, thereby constraining these ignored objects to yield higher influence towards model predictions. More importantly, this influence can be seamlessly transferred to the attention weights learning since these two are positively correlated (refer to Figure 2 (b)). As such, the attention weight improvement of ignored key objects can be eventually achieved.

On the other hand, by training the model with $\langle Q, I^m, \hat{A}^m \rangle$ and $\langle Q, I, \hat{A} \rangle$ simultaneously, the existence of the masked visual information (i.e., ignored key objects) would be strengthened as a necessary condition for predicting the correct answers, as illustrated in Figure 3 (b). Hence, the strong correlation between the ignored key objects and the ground-truth answers can be built under this situation. The training algorithm of our method is summarized at Algorithm 2.

Overall, we optimize the parameters in our model by simultaneously training with the original and curated samples,

$$\mathcal{L}_{all} = \mathcal{L}_{vqa} + \lambda \mathcal{L}_{reg}, \quad (6)$$

where \mathcal{L}_{vqa} and \mathcal{L}_{reg} respectively denote the original sample training loss and curated sample training loss, and λ is a hyper-parameter to control the regularization strength. In the testing phase, the regularization module is no longer activated and only the backbone model remains.

4 EXPERIMENTS

4.1 Datasets and Experimental Settings

4.1.1 Datasets. We evaluated the proposed AttReg mainly on the diagnostic VQA-CP datasets [1], wherein the answer distributions for each question category in the training and testing sets are significantly different. As such, most VQA models that lack visual grounding ability and rely on superficial correlations between questions and answers (*i.e.*, language biases) would perform poorly on this dataset. The experimental results on the VQA v2 [13] are also reported for completeness.

4.1.2 Evaluation Metrics. We adopted the standard VQA accuracy metric [4] to evaluate the model performance, which is defined as,

$$ACC(ans) = \min \left\{ 1, \frac{\text{\#humans that provide } ans}{3} \right\}. \quad (7)$$

Note that each question is answered by ten annotators, and ACC considers the disagreement among human answers.

4.1.3 Implementation and Training Details. We implemented our method following the preprocessing steps of the widely-adopted UpDn model [2] as well as the LMH model [9] for a fair comparison. Specifically, for each image, the UpDn utilizes Faster-RCNN to generate 36 object proposals as the visual features, *i.e.*, a 2,048-d vector for each object. All the questions are converted to lower case and trimmed to a maximum of 14 words. And the questions with less than 14 words are padded with zeros. The pre-trained GloVe vectors are used to initialize the word embedding matrix, *i.e.*, a 300-d vector for each word. And then a single-layer GRU is employed to obtain sentence-level question encoding of 512-d.

We first pretrained the backbone model on the training splits using the plain VQA loss \mathcal{L}_{vqa} . We then regularized the visual attention for the backbone model by fine-tuning with \mathcal{L}_{all} in Eqn. (6). For UpDn and LMH, the learning rate is set to $2e-3$ during pre-training, and reduced to $2e-5$ and $2e-4$ when fine-tuning, respectively. In addition, the number of the key objects M is tuned between 1 and 6. And for the ignored objects, the proportion of $N\%$ is tuned between 10% and 40%.

4.2 Comparisons with State-of-the-Arts

4.2.1 Performance on VQA-CP v2 and VQA v2. Table 2 exhibits the results of our method and the SOTA VQA models on VQA-CP v2 and VQA v2. The first part in this table exhibits typical VQA models, followed by the models designed to overcome superficial biases. And the last two parts denote the backbone models with or without visual grounding enhancement methods, *i.e.*, SCR [28], HINT [26], AttAlign [26], CSS [7], and our AttReg. Table 3 illustrates the test results of our method on the VQA v2 test set³. The main observations are as follows.

Firstly, our LMH-AttReg achieves a new state-of-the-art performance of 59.92% ACC on the VQA-CP v2 dataset. Specifically, in the ‘Yes/No’ and ‘Number’ answer categories, the LMH-AttReg achieves 2.91% and 2.97% improvements over the existing best approach LMH-CSS, respectively.

Secondly, our AttReg dramatically improves the backbone model performance on the VQA-CP v2 dataset. By incorporating AttReg into UpDn, a large improvement is achieved (*i.e.*, +6.76%). And LMH-AttReg also yields a large gain (*i.e.*, +6.93%) over its backbone LMH, which highlights the effectiveness and the generalization capability of AttReg.

Thirdly, our AttReg can enhance the backbone model performance on the VQA v2 dataset over all answer categories. In contrast, most approaches that perform well on VQA-CP v2 suffer

³The test results of LMH and LMH-AttReg are not available. This is because the VQA v2 testing set does not provide the question type information for each question, which are indispensable for these two models.

Table 2. Performance comparison between the proposed method and the state-of-the-arts on VQA-CP v2 test and VQA v2 val. *Expl.* implies the source of the explanations, e.g., human attention (HAT) [10]. *Att.* represents the visual attention regularization approach. *Grad.* stands for the Grad-CAM methods. [†] denotes our implementation. The mean score represents the accuracy average on VQA-CP v2 and VQA v2.

Method	Expl.	Att.	Grad.	VQA-CP v2 test				VQA v2 val				Mean	
				All	Yes/No	Number	Other	All	Yes/No	Number	Other	All	Yes/No
SAN [31]				24.96	38.35	11.14	21.74	52.41	70.06	39.28	47.84	38.69	54.21
NMN [3]				27.47	38.94	11.92	25.72	51.62	73.38	33.23	39.93	39.55	56.16
HAN [18]				28.65	52.25	13.79	20.33	-	-	-	-	-	-
MCB [12]				36.33	41.01	11.96	40.57	59.71	77.91	37.47	51.76	48.02	59.46
GVQA [1]				31.30	57.99	13.68	22.14	48.24	72.03	31.17	34.65	39.77	65.01
MuRel [5]				39.54	42.85	13.17	45.04	-	-	-	-	-	-
AdvReg [22]				41.17	65.49	15.48	35.48	62.75	79.84	42.35	55.16	51.96	72.67
RUBi [6]				47.11	68.65	20.28	43.18	61.16	-	-	-	54.14	-
UpDn [†] [2]				40.09	42.16	12.36	46.61	63.77	81.54	43.64	55.59	51.93	61.85
UpDn-SCR [28]	QA		✓	48.74	70.41	10.42	47.29	62.30	77.40	40.90	56.50	55.39	73.91
UpDn-HINT [26]	HAT		✓	46.73	67.27	10.61	45.88	63.38	81.18	42.99	55.56	55.06	74.23
UpDn-AttAlign [26]	HAT	✓		39.37	43.02	11.89	45.00	63.24	80.99	42.55	55.22	51.31	62.01
UpDn-AttReg (Ours)	QA	✓		46.85	69.34	12.44	44.51	64.13	81.72	43.77	56.13	55.49	75.53
LMH [†] [9]				52.99	72.02	39.24	46.79	62.40	79.42	41.48	54.99	57.70	75.72
LMH-CSS [7]	QA		✓	58.95	84.37	49.42	48.21	59.91	73.25	39.77	55.11	59.43	78.81
LMH-AttReg (Ours)	QA	✓		59.92	87.28	52.39	47.65	62.74	79.71	41.68	55.42	61.33	83.50

performance drop over this dataset. For example, introducing SCR [28] into UpDn leads to a significant improvement of +8.65% on VQA-CP v2; whereas the -1.47% performance drop can be observed when SCR works on VQA v2. By comparison, AttReg can enhance UpDn on both VQA-CP v2 (+6.76%) and VQA v2 (+0.36%), which further reveals the robustness of AttReg.

Fourthly, we compared our AttReg with a straightforward visual attention regularization method – AttAlign [26], which directly aligns visual attention with human attentions. The result demonstrates that our AttReg outperforms AttAlign with a large margin on the two datasets, especially on VQA-CP v2 (46.85% vs. 39.37%). This proves the effectiveness and superiority of our method among the visual attention regularization ones.

Lastly, we equipped existing gradient-based regularization methods (*i.e.*, Grad-CAM methods) into the well-devised UpDn model to evaluate their effectiveness, and compared with our AttReg. It can be found that while these Grad-CAM methods enhance model performance significantly on VQA-CP v2, they usually deteriorate the backbone model performance on VQA v2. Instead, our AttReg is able to not only improve the model performance on the two datasets, but also achieve the highest mean score over the two datasets among the existing grounding enhancement approaches, *i.e.*, LMH-AttReg vs. LMH-CSS (61.33% vs. 59.43%) and UpDn-AttReg vs. UpDn-SCR (55.49% vs. 55.39%). This further proves our previous finding (in Section 2): visual attention is more faithful to model decisions. In this way, a favorable visual attention regularization approach can yield more robust enhancement over the backbone model.

4.2.2 Performance on VQA-CP v1. Table 4 shows the results of our method and the SOTA VQA models on the VQA-CP v1 dataset. Similarly, we group these models into: i) typical VQA models; ii) models designed to overcome superficial biases; and iii) the backbone models with and without visual grounding enhancement methods, *i.e.*, CSS and our AttReg. From the results, we can observe that our LMH-AttReg achieves a new state-of-the-art performance on VQA-CP v1. In addition, our AttReg significantly improves the backbone performance on VQA-CP v1, *i.e.*, +6.52% on LMH and +8.78% on UpDn.

Table 3. Performance of the proposed method on VQA v2 test-std. [†] denotes our implementation.

Method	All	Yes/No	Number	Other
UpDn [†] [2]	64.90	81.82	42.73	55.51
UpDn-AttReg (Ours)	65.25	82.18	43.68	55.71

Table 4. Performance comparison between the proposed method and the state-of-the-arts on the VQA-CP v1 test set.

Method	All	Yes/No	Number	Other
SAN [31]	26.88	35.34	11.34	24.70
NMN [3]	29.64	38.85	11.23	27.88
MCB [12]	34.39	37.96	11.80	39.90
GVQA [1]	39.23	64.72	11.87	24.86
AdvReg [22]	43.43	74.16	12.44	25.32
RUBi [6]	50.90	80.83	13.84	36.02
UpDn [†] [2]	38.88	42.48	13.12	45.66
UpDn-AttReg (Ours)	47.66	66.17	12.11	43.54
LMH [†] [9]	55.73	78.59	24.68	45.47
LMH-CSS [7]	60.95	85.60	40.57	44.62
LMH-AttReg (Ours)	62.25	88.29	35.30	47.18

4.3 Parameter Analyses

4.3.1 The Regularization Strength λ . Table 5 summarizes the effect of varying regularization strength of \mathcal{L}_{reg} on two backbone models. From the results, we observed that the best performance is achieved when $\lambda = 5$ and $\lambda = 0.5$ for UpDn and LMH, respectively. Note that for small values of λ , the regularization takes less effect and the backbone model continues to ignore the key objects for answering. On the other hand, when λ becomes too large, the ignored key objects would impose too much impact on answer prediction, while leaving the other important context cues uninvolved. Both cases would degrade the final model performance.

4.3.2 The Size of Key Objects V^* . To evaluate the influence of $|V^*|$, we varied it from 1 to 6 to train our model with different settings on the VQA-CP v2 dataset and reported the results in Figure 4 (a). It can be observed that the model accuracy obtains enhancement with a larger size of V^* but deteriorates at some points, e.g., $|V^*| = 6$. The reason is that the image often contains certain number of key objects, and therefore the performance is promoted when more key objects are considered. Nonetheless, the objects with lower similarities with QA pairs can also be included when $|V^*|$ is too large. This would introduce noise into the identified key objects and deteriorate the AttReg's effect.

4.3.3 The Size of Deemed Ignored Objects V^o . As aforementioned, we took the objects whose attention weights are out of top- $N\%$ as the ignored objects V^o . Thus, we compared the performance variation of different proportions of top- $N\%$ to evaluate the influence of $|V^o|$. As shown in Figure 4 (a), our AttReg can achieve better performance when more objects with low attention weights are included in V^o , e.g., out of top-10%. In fact, this is consistent with our previous finding in Table 1 – most image objects with low attention weights are ignored by the model because they hardly impose an effect on model predictions. Consequently, when the majority of these kind of objects

Table 5. The influence of the regularization strength of AttReg on two backbones over VQA-CP v2 test.

Method	λ	All	Yes/No	Number	Other
UpDn	-	40.09	42.16	12.36	46.61
UpDn-AttReg	0.5	45.53	61.43	12.11	46.37
UpDn-AttReg	1	46.75	66.23	11.94	46.09
UpDn-AttReg	5	46.85	69.34	12.44	44.51
UpDn-AttReg	20	46.49	67.14	12.82	44.91
LMH	-	52.99	72.02	39.24	46.79
LMH-AttReg	0.1	57.20	81.68	46.25	47.37
LMH-AttReg	0.5	59.92	87.28	52.39	47.65
LMH-AttReg	1	58.69	82.78	52.94	47.63
LMH-AttReg	5	55.74	76.16	51.78	46.14

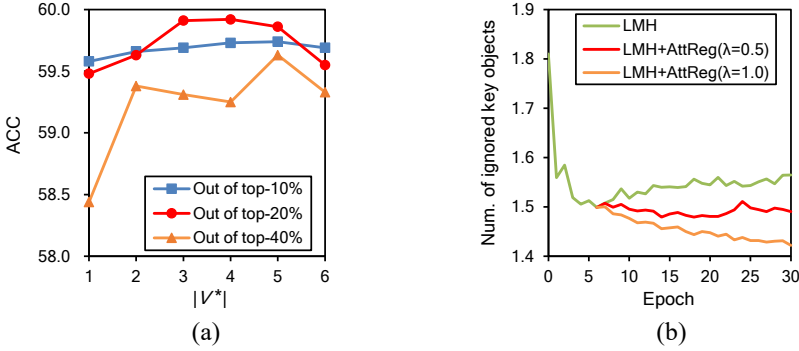


Fig. 4. (a) The ACC curves with respect to different sizes of V^* and the proportion of the deemed ignored objects. All results are obtained from the LMH-AttReg. (b) The number of ignored key objects regarding the training epochs of LMH and LMH-AttReg. Note that the AttReg is introduced to fine-tune the backbone LMH after 7 epochs.

are included in V^o , the missed ignored objects in the locating process would be fewer and our AttReg can work better under this situation.

4.4 Effectiveness in Improving Visual Attention

4.4.1 Quantitative Evaluation. Figure 4 (b) shows how the number of ignored key objects changes with the increase of training steps. It can be seen that the number of ignored key objects assigned by the visual attention in the baseline LMH is continuously increasing with more training iterations after epoch 7. In contrast, this number is decreasing when the visual attention is guided by our AttReg, especially when the regularization strength of AttReg becomes stronger. This demonstrates the effectiveness of AttReg in regularizing the visual attention to focus more on the ignored key objects.

To more intuitively understand the improvement of visual attention, we conducted ablation studies and calculated the performance gap for the backbone model with or without the visual attention module. As shown in Table 6, we can observe that the performance gap becomes larger if

Table 6. Influence of the visual attention module on VQA-CP v2 and VQA v2 datasets. Gap Δ denotes the performance variation in comparison with the baseline.

	Method	VQA-CP v2		VQA v2	
		All	Gap Δ	All	Gap Δ
UpDn	Baseline	40.09	-	63.77	-
	w/o VAtt	29.62	10.47	51.87	11.9
UpDn-AttReg	Baseline	46.85	-	64.13	-
	w/o VAtt	35.34	11.51	51.88	12.25

the visual attention is regularized by our AttReg, showing that the visual attention module plays a more pivotal role in model performance enhancement.

4.4.2 Qualitative Evaluation. To better illustrate the effectiveness of AttReg, we visualized the attention maps generated by the backbones with and without our AttReg, and exhibited the results in Figure 5. In all cases, the backbone model shifts more attention to the ignored key objects after introducing our AttReg. And the model is also promoted to predict the right answer with the correct visual grounding. Take the left one as an example, with our AttReg, the attention weight of the ignored key object *dress* grows from 0.00 to 0.33, and becomes the most influential one among all objects in the image, which further help to yield the correct answer of *blue*.

5 RELATED WORK

In this section, we discuss two categories which are closely related to this work: visual attention in VQA and visual grounding enhancement for VQA.

5.1 Visual Attention in VQA

Visual attention has raised more and more concern over the past few years owing to its effectiveness and explanatory capacity. At the very beginning, the visual attention is introduced into VQA to address the “where to look” problem by directly calculating the semantic similarity between the question and image regions [27]. To obtain more fine-grained visual representation, [17] and [30] later applied the hierarchical question structure modeling for image attention. The question representations are learned from multi-levels, *e.g.*, word-level and phrase-level, which are effectively employed to conduct visual attention recursively. In addition, the multi-glimpse visual attention mechanism [31] is subsequently proposed to iteratively infer the answer by attending on visual features multiple times. Different from the above top-down visual attention methods, Anderson et al. [2] presented a combined bottom-up and top-down attention mechanism (UpDn) which firstly detects common objects and attributes in an image and then leverages visual attention to attend on these high-level concepts. This technique has been widely adopted and extended in recent studies [6, 7, 28], boosting the performance of a series of VQA models.

However, the above visual attention-based models are all restricted by the lack of guidance for visual grounding [10, 26]. Training with implicit optimizing protocols, these VQA models do not receive any guidance in visual grounding, and therefore are inclined to focus on irrelevant visual contents or even resort to superficial biases to answer questions. To address this problem, in this work, we present a novel regularization strategy to guide the attention learning and boost the answer prediction accuracy.

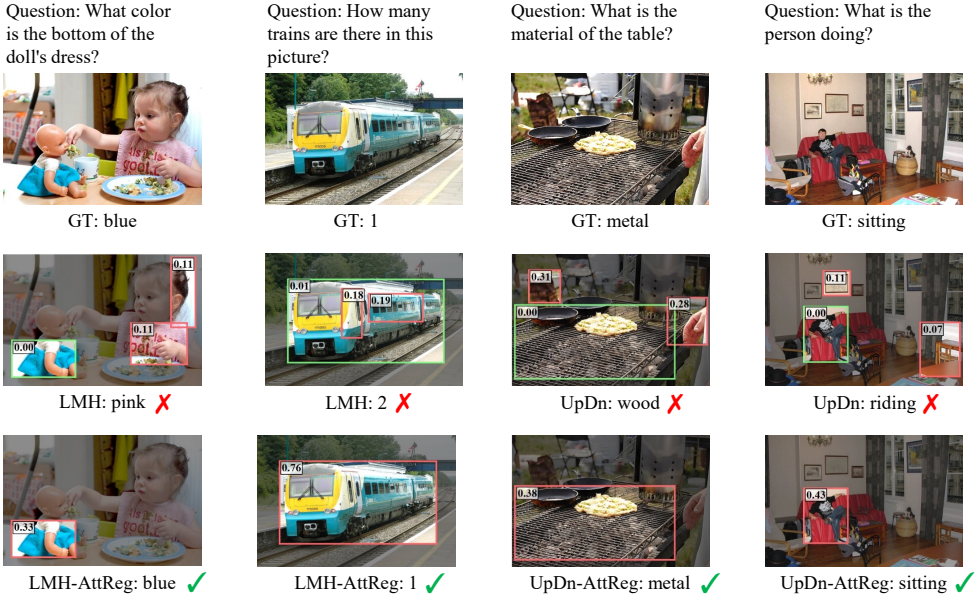


Fig. 5. Visualization of two backbone models with and without AttReg. The green boxes denote the ignored key objects and the pink ones represent the objects with highest attention weights. The value around the bounding box is the visual attention weight to the given object.

5.2 Visual Grounding Enhancement for VQA

One of the most desired properties for VQA systems is to equip correct visual grounding for model decisions, *i.e.*, right for right reasons [24, 28]. Existing approaches for this purpose can be roughly classified into two groups: 1) visual attention; and 2) Grad-CAM ones. Visual attention methods [21, 34] target at aligning the attention weights with explicit human attentions. Since the human attention data are far too expensive and difficult to collect, the practicability and generalization of these techniques are largely limited.

In contrast, Grad-CAM approaches derive the gradient value of each image region from the model predictions to achieve visual grounding. For example, Selvaraju et al. [26] presented a human importance-aware network tuning (HINT) to enforce the gradient-based importance to share the same ranking with the human attention map. SCR [28] leverages the textual annotations (*e.g.*, QA pairs) to relate with the influential regions in images first, and then criticizes the incorrect answers' sensitivity to these regions. More recently, Chen et al. [7] designed a Counterfactual Samples Synthesizing (CSS) scheme which guides the model to answer questions based on critical contents (*e.g.*, the image regions with high gradient importance to ground-truth answers) by training the model with the generated complementary samples. Different from the above ones, Patro et al. [19] devised an adversarial learning strategy to guide attention maps by utilizing the Grad-CAM results as the surrogate supervision. However, our experiments reveal that the Grad-CAM visual explanations are not closely related to the answer prediction, which limits its visual grounding capability to some extent.

6 CONCLUSION AND FUTURE WORK

In this work, we present a model agnostic visual attention regularization approach, *i.e.*, AttReg, to guide the attention learning in VQA. AttReg has been applied to two strong baselines and significantly improves the backbone model performance over the VQA-CP v2 and VQA-CP v1 datasets. As a by-product, AttReg achieves a new state-of-the-art performance on VQA-CP v2. In addition, we also empirically study the faithfulness of visual attention in VQA. The experimental results have demonstrated that visual attention methods obviously outperform the Grad-CAM ones in terms of visual grounding.

In the future, we will extend our approach to other tasks which are also hindered by the unsupervised attention learning problems, *e.g.*, image captioning.

REFERENCES

- [1] Aishwarya Agrawal, Dhruv Batra, Devi Parikh, and Aniruddha Kembhavi. 2018. Don't just assume; look and answer: Overcoming priors for visual question answering. In *Proceedings of the IEEE Conference on Computer Vision and Pattern Recognition*. IEEE, 4971–4980.
- [2] Peter Anderson, Xiaodong He, Chris Buehler, Damien Teney, Mark Johnson, Stephen Gould, and Lei Zhang. 2018. Bottom-up and top-down attention for image captioning and visual question answering. In *Proceedings of the IEEE Conference on Computer Vision and Pattern Recognition*. IEEE, 6077–6086.
- [3] Jacob Andreas, Marcus Rohrbach, Trevor Darrell, and Dan Klein. 2016. Deep compositional question answering with neural module networks. In *Proceedings of the IEEE Conference on Computer Vision and Pattern Recognition*. IEEE, 39–48.
- [4] Stanislaw Antol, Aishwarya Agrawal, Jiasen Lu, Margaret Mitchell, Dhruv Batra, C Lawrence Zitnick, and Devi Parikh. 2015. Vqa: Visual question answering. In *Proceedings of IEEE International Conference on Computer Vision*. IEEE, 2425–2433.
- [5] Remi Cadene, Hedi Ben-younes, Matthieu Cord, and Nicolas Thome. 2019. MuRel: Multimodal relational reasoning for visual question answering. In *Proceedings of the IEEE Conference on Computer Vision and Pattern Recognition*. IEEE, 1989–1998.
- [6] Remi Cadene, Corentin Dancette, Hedi Ben-younes, Matthieu Cord, and Devi Parikh. 2019. Rubi: Reducing unimodal biases in visual question answering. In *Proceedings of Advances in Neural Information Processing Systems*. Curran Associates, Inc., 839–850.
- [7] Long Chen, Xin Yan, Jun Xiao, Hanwang Zhang, Shiliang Pu, and Yueting Zhuang. 2020. Counterfactual samples synthesizing for robust visual question answering. In *Proceedings of the IEEE Conference on Computer Vision and Pattern Recognition*. IEEE, 10800–10809.
- [8] Kyunghyun Cho, Bart van Merriënboer, Caglar Gulcehre, Dzmitry Bahdanau, Fethi Bougares, Holger Schwenk, and Yoshua Bengio. 2014. Learning phrase representations using RNN Encoder-Decoder for statistical machine translation. In *Proceedings of the Conference on Empirical Methods in Natural Language Processing*. ACL, 1724–1734.
- [9] Christopher Clark, Mark Yatskar, and Luke Zettlemoyer. 2019. Don't take the easy way out: Ensemble based methods for avoiding known dataset biases. In *Proceedings of the Conference on Empirical Methods in Natural Language Processing*. ACL, 4069–4082.
- [10] Abhishek Das, Harsh Agrawal, C. Lawrence Zitnick, Devi Parikh, and Dhruv Batra. 2016. Human attention in visual question answering: Do humans and deep networks look at the same regions?. In *Proceedings of the Conference on Empirical Methods in Natural Language Processing*. ACL, 932–937.
- [11] Zhiwei Fang, Jing Liu, Xueliang Liu, Qu Tang, Yong Li, and Hanqing Lu. 2019. BTDP: Toward sparse fusion with block term decomposition pooling for visual question answering. *ACM Trans. Multimedia Comput. Commun. Appl.* 15, 50 (2019), 1–21. Issue 2s.
- [12] Akira Fukui, Dong Huk Park, Daylen Yang, Anna Rohrbach, Trevor Darrell, and Marcus Rohrbach. 2016. Multimodal compact bilinear pooling for visual question answering and visual grounding. In *Proceedings of the Conference on Empirical Methods in Natural Language Processing*. ACL, 457–468.
- [13] Yash Goyal, Tejas Khot, Douglas Summers-Stay, Dhruv Batra, and Devi Parikh. 2017. Making the V in VQA matter: Elevating the role of image understanding in visual question answering. In *Proceedings of the IEEE Conference on Computer Vision and Pattern Recognition*. IEEE, 6325–6334.
- [14] Matthew Honnibal, Ines Montani, Sofie Van Landeghem, and Adriane Boyd. 2020. *spaCy: Industrial-strength Natural Language Processing in Python*. <https://doi.org/10.5281/zenodo.1212303>

- [15] Sarthak Jain and Byron C. Wallace. 2019. Attention is not Explanation. In *Proceedings of the 2019 Conference of the North American Chapter of the Association for Computational Linguistics: Human Language Technologies*. ACL, 3543–3556.
- [16] Qun Li, Fu Xiao, Le An, Xianzhong Long, and Xiaochuan Sun. 2019. Semantic concept network and deep walk-based visual question answering. *ACM Trans. Multimedia Comput. Commun. Appl.* 15, 49 (2019), 1–19. Issue 2s.
- [17] Jiasen Lu, Jianwei Yang, Dhruv Batra, and Devi Parikh. 2016. Hierarchical question-image co-attention for visual question answering. In *Proceedings of Advances in Neural Information Processing Systems*. Curran Associates, Inc., 289–297.
- [18] Mateusz Malinowski, Carl Doersch, Adam Santoro, and Peter Battaglia. 2018. Learning visual question answering by bootstrapping hard attention. In *Proceedings of European Conference on Computer Vision*. Springer, 3–20.
- [19] Badri N. Patro, Anupriy, and Vinay P. Nambodiri. 2020. Explanation vs attention: A two-player game to obtain attention for VQA. In *Proceedings of the Conference on Artificial Intelligence*. AAAI Press, 11848–11855.
- [20] Jeffrey Pennington, Richard Socher, and Christopher Manning. 2014. GloVe: Global vectors for word representation. In *Proceedings of the Conference on Empirical Methods in Natural Language Processing*. ACL, 1532–1543.
- [21] Tingting Qiao, Jianfeng Dong, and Duanqing Xu. 2018. Exploring human-Like attention supervision in visual question answering. In *Proceedings of the Conference on Artificial Intelligence*. AAAI Press, 7300–7307.
- [22] Sainandan Ramakrishnan, Aishwarya Agrawal, and Stefan Lee. 2018. Overcoming language priors in visual question answering with adversarial regularization. In *Proceedings of Advances in Neural Information Processing Systems*. Curran Associates, Inc., 1548–1558.
- [23] Shaoqing Ren, Kaiming He, Ross Girshick, and Jian Sun. 2015. Faster r-cnn: Towards real-time object detection with region proposal networks. In *Proceedings of Advances in Neural Information Processing Systems*. Curran Associates, Inc., 91–99.
- [24] Andrew Slavin Ross, Michael C. Hughes, and Finale Doshi-Velez. 2017. Right for the right reasons: Training differentiable models by constraining their explanations. In *Proceedings of the International Joint Conference on Artificial Intelligence*. AAAI Press, 2662–2670.
- [25] Ramprasaath R. Selvaraju, Michael Cogswell, Abhishek Das, Ramakrishna Vedantam, Devi Parikh, and Dhruv Batra. 2017. Grad-CAM: Visual explanations from deep networks via gradient-based localization. In *Proceedings of IEEE International Conference on Computer Vision*. IEEE, 618–626.
- [26] Ramprasaath R. Selvaraju, Stefan Lee, Yilin Shen, Hongxia Jin, Shalini Ghosh, Larry Heck, Dhruv Batra, and Devi Parikh. 2019. Taking a hint: Leveraging explanations to make vision and language models more grounded. In *Proceedings of IEEE International Conference on Computer Vision*. IEEE, 2591–2600.
- [27] Kevin J. Shih, Saurabh Singh, and Derek Hoiem. 2016. Where to look: Focus regions for visual question answering. In *Proceedings of the IEEE Conference on Computer Vision and Pattern Recognition*. IEEE, 4613–4621.
- [28] Jialin Wu and Raymond J. Mooney. 2019. Self-critical reasoning for robust visual question answering. In *Proceedings of Advances in Neural Information Processing Systems*. Curran Associates, Inc., 8601–8611.
- [29] Qi Wu, Damien Teney, Peng Wang, Chunhua Shen, Anthony Dick, and Anton van den Hengel. 2017. Visual question answering: A survey of methods and datasets. *Computer Vision and Image Understanding* 163 (2017), 21–40.
- [30] Huijuan Xu and Kate Saenko. 2016. Ask, attend and answer: Exploring question-guided spatial attention for visual question answering. In *Proceedings of European Conference on Computer Vision*. Springer, 451–466.
- [31] Zichao Yang, Xiaodong He, Jianfeng Gao, Li Deng, and Alex Smola. 2016. Stacked attention networks for image question answering. In *Proceedings of the IEEE Conference on Computer Vision and Pattern Recognition*. IEEE, 21–29.
- [32] Dongfei Yu, Jianlong Fu, Xinmei Tian, and Tao Mei. 2019. Multi-source multi-level attention networks for visual question answering. *ACM Trans. Multimedia Comput. Commun. Appl.* 15, 51 (2019), 1–20. Issue 2s.
- [33] Peng Zhang, Yash Goyal, Douglas Summers-Stay, Dhruv Batra, and Devi Parikh. 2016. Yin and yang: Balancing and answering binary visual questions. In *Proceedings of Advances in Neural Information Processing Systems*. Curran Associates, Inc., 5014–5022.
- [34] Yundong Zhang, Juan Carlos Niebles, and Alvaro Soto. 2019. Interpretable visual question answering by visual grounding from attention supervision mining. In *Proceedings of the IEEE Winter Conference on Applications of Computer Vision*. IEEE, 349–357.